Statistical analysis of noise-induced multiple filamentation

J. Garnier*
Laboratoire de Probabilités et Modèles Aléatoires & Laboratoire Jacques-Louis Lions, Université Paris VII, 2 Place Jussieu, 75251 Paris Cedex 5, France
(Received 14 February 2006; published 26 April 2006)

The propagation of high-power large-aperture laser beams in a Kerr medium is considered. A statistical approach is developed for the growth of filaments from small-amplitude small-scale initial modulations. Closed-form expressions are derived for the intensity distribution, contrast, and maximal beam intensity, which are valid up to the blowup of the most intense filament. Numerical experiments are found to be in good agreement with theoretical predictions.

DOI: 10.1103/PhysRevE.73.046611 PACS number(s): 42.65.Tg, 42.65.Jx

I. INTRODUCTION

It is well known that noise in an input high-power laser beam may lead to multiple filamentation [1]. Many self-focusing experiments in solids, liquids, and gases have shown that a single input beam breaks up into several long and narrow filaments [2–10]. This paper presents a quantitative analysis of the filament growth in high-power large-aperture laser beams propagating in a Kerr-like medium. It is based on a statistical study of the nonlinear Schrödinger (NLS) equation with a random initial condition. This work is first motivated by inertial confinement fusion (ICF) concern. The growth of laser damage is one of the major limitations to the lifetime of optics on high-power laser chains, especially Megajoule-class laser LIL (Ligne d'Intégration Laser), LMJ (Laser MégaJoule), or NIF (National Ignition Facility) [11,12]. Thick windows are necessary in laser chains to close safely spatial filters or interaction chambers. Fluences and powers far exceed the threshold power values for self-focusing, so it is critical to control the growth of filaments. We aim at predicting the growth of filaments by studying the multiple filamentation of large-aperture beams with small-scale modulations. Of course the results obtained in this paper are not specific to ICF and could be applied to other situations—for instance, to propagation of intense laser beams in plasma [13].

In ICF configurations the pulse duration is large, of the order of a few nanoseconds, so that group velocity dispersion can be neglected. The total beam power is much larger than the critical self-focusing power, the beam is large (several millimeters, centimeters, or tens of centimeters in diameter), and it possesses a flat-top profile (see, for instance, [14]). As a result the self-focusing distance of the beam is much larger than the typical propagation distance. However, the beam transverse profile is not perfect and it actually possesses small-scale fluctuations in amplitude and phase. These small perturbations can cause self-focusing of small sections of the beam. At some point the irradiance is high enough to damage the material, and this catastrophic self-focusing represents a major risk that must be considered in the design of ICF lasers. The resolution of these small scales makes modeling calculationally intensive, although possible with present tools [15]. However, practitioners would like to possess more efficient tools in order to estimate the filamentation risk. The initial fluctuations have small sizes and small standard deviations, typically a few percent of the average [14]. The early steps of the propagation can then be analyzed using modulation theory according to the well-known Bespalov-Talanov theory [1]. This regime is characterized by the exponential growth of the modulation modes with a growth rate that depends on the transverse spatial wave number. Multiple filamentation can be predicted by this theory because the exponential growth of oscillatory modulations is likely to break the beam into small-scale cells, and thus multiple filaments can emerge [16,17]. However, this approach consists of a linear stability analysis, so that it holds as long as the intensity modulations remain smaller than the mean intensity. Our aim is to go beyond this regime and to analyze quantitatively the growths of filaments.

The first step consists of a weakly nonlinear (WNL) analysis where mode coupling takes place. Indeed, when the modulation amplitude reaches a critical value that can be computed, mode coupling becomes possible between a broad range of transverse frequencies and wave numbers. The results of these WNL interactions strongly depend on the modes that dominate the modulation spectrum just before the transition from the linear regime to the WNL regime. One of the main issues is whether the dynamics is dominated by the mode with the largest initial amplitude or by the mode with the largest linear growth rate. The answer to this question has dramatic consequences on the WNL regime.

The WNL analysis in many respects reproduces well-known results of the weak-turbulence theory [18], but this paper goes far beyond. The WNL regime is in fact an intermediate regime between the linear regime and the fully nonlinear (FNL) regime characterized by the growth of filaments. Once again, the transition between these regimes can be analyzed, and the initial conditions for the FNL regime are given by the final state of the WNL regime. We shall see that the FNL regime can be described as the growth of independent hot spots whose initial configurations can be described statistically. As a result the statistical distribution of the number and intensities of filaments can be studied.

The paper is organized as follows. Section II describes the modulation theory for multimode modulations. We insist on

*Electronic address: garnier@math.jussieu.fr

the relevance of the statistical approach that is proposed for the modeling of the initial beam modulations. We then perform a WNL analysis. Section IV gives formulas for the intensity distribution and contrast. Section V addresses the growth of the most intense filaments, and our theoretical predictions are compared with full numerical simulations of the NLS equation in Sec. VII.

II. NONLINEAR PROPAGATION OF AN INTENSE BEAM

We address the propagation of a monochromatic laser beam along the z axis. We take into account the effects of diffraction and Kerr nonlinearity. The evolution of the slowly varying envelope is then governed by the NLS equation [19]

$$i\frac{\partial E}{\partial z}+\frac{1}{2k_0}\Delta_\perp E+\gamma|E|^2E=0, \tag{1}$$

where $\Delta_\perp=\frac{\partial^2}{\partial x^2}+\frac{\partial^2}{\partial y^2}$ is the transverse Laplacian. The nonlinear coefficient is $\gamma=(k_0n_{2E})/(2n_0)$, n_0 is the linear index of refraction, and n_{2E} is the Kerr coefficient that models the response of the medium to the electric field. $k_0=2\pi n_0/\lambda$ is the homogeneous wave number. The laser intensity I_{laser} (i.e., the power per area unit) is proportional to the square modulus of the complex electric field, $I_{laser}=\epsilon_0n_0c|E|^2/2$, and the usual parameter n_2 is related to n_{2E} through the identity $n_{2E}|E|^2/2=n_2I_{laser}$. We thus have $\gamma=n_2k_0\epsilon_0c/2$. The typical values for glass are $n_0\simeq1.55$ and $n_2\simeq2.7\times10^{-7}$ cm^2/GW.

The NLS equation possesses plane-wave solutions

$$E_{ref}(z,\mathbf{r})=\sqrt{I_0}\exp(i\gamma I_0z). \tag{2}$$

Let us introduce some noise in the initial conditions

$$E(z=0,\mathbf{r})=\sqrt{I_0}[1+q_0(\mathbf{r})].$$

We model the initial amplitude and phase modulations $q_0(\mathbf{r})$ as the realization of a spatially random process with Gaussian statistics. The statistical distribution of this process is characterized by the two first moments

$$\langle q_0(\mathbf{r})\rangle=0,\quad \langle q_0(\mathbf{r}')q_0^*(\mathbf{r})\rangle=C(\mathbf{r}-\mathbf{r}'),$$

where the brackets stand for a statistical average and C is the so-called autocorrelation function. The autocorrelation function of the Fourier transform of q_0 is

$$\langle\hat{q}_0(\mathbf{k}')\hat{q}_0^*(\mathbf{k})\rangle=\Gamma_{q_0}(\mathbf{k})\delta(\mathbf{k}'-\mathbf{k}).$$

The positive-valued function $\mathbf{k}\mapsto\Gamma_{q_0}(\mathbf{k})$ is the power spectral density (PSD) defined by

$$\Gamma_{q_0}(\mathbf{k})=\int C(\mathbf{r})\exp(-i\mathbf{k}\cdot\mathbf{r})d^2\mathbf{r}.$$

A limit case is the white noise model where the correlation radius of the process is assumed to be very small. The autocorrelation function can then be reduced to a Dirac distribution $C(\mathbf{x})=\Gamma_0\delta(\mathbf{x})$ and the PSD is identically equal to the constant Γ_0.

The choice of a statistical description for the multimode modulation is both mathematically and physically relevant. Indeed the initial modulations are only known approximately. The statistical model takes into account the available data (rms, spectrum) and completes the unknown data by putting a statistical distribution on them. This distribution should be chosen in a natural way, and the most natural model (maximizing the entropy) when only the first two moments are specified is Gaussian statistics. Finally, the choice of Gaussian statistics is also consistent with the empirical picture that the initial modulations originate from many small imperfections: we can then invoke the central limit theorem which claims that Gaussian statistics always results from the contribution of many independent effects [20]. To be complete we should add that this model is correct for spatially uniformly distributed defects (which is the case encountered in ICF configurations for instance), but some special configurations do not fit into the model. Here we think of the defect perturbations proposed in [21] where a multiplicative factor reinforces the beam amplitude at a point or along a line.

We seek a solution in the form

$$E(z,\mathbf{r})=E_{ref}(z,\mathbf{r})[1+q(z,\mathbf{r})], \tag{3}$$

where the modulation is denoted by $q(z,\mathbf{r})$ whose Fourier components (with respect to the transverse spatial variables $\mathbf{r}$) are

$$\hat{q}(z,\mathbf{k})=\frac{1}{2\pi}\int d^2\mathbf{r}\exp(-i\mathbf{k}\cdot\mathbf{r})q(z,\mathbf{r}),\quad \mathbf{k}\in\mathbb{R}^2.$$

We shall first compute the PSD of q which is proportional to the average square modulus of the Fourier components $\langle|\hat{q}(z,\mathbf{k})|^2\rangle$. More specifically we shall seek information about the intensity distribution of the total field E defined by $|E|^2(z,\mathbf{r})=I_0|1+q(z,\mathbf{r})|^2$. In particular we would like to compute the contrast, the intensity distribution, and the distribution of the number and intensities of the filaments.

Before introducing the equations governing the dynamics, we would like to comment on the interpretation of the results. We consider a set of possible realizations of the initial modulations. From a practical point of view we seek information that holds true for an arbitrary realization of the initial modulations. We are going to compute statistical averages. Throughout the paper we focus our attention on the PSD of the modulation. This function actually contains all the information about the spatial process q [20]. The ergodic principle gives the equivalence between the theoretical statistical average and the experimental local or global spatial averages, such as the spatial spectrum or the rms. Actually, the statistical theory provides much more accurate results depending only on the PSD. For instance, the local shape of a local maximum can be computed theoretically, as well as the density of local maxima above a given value, etc. [20].

III. WEAKLY NONLINEAR ANALYSIS

A. Linear regime

The study of the linear regime is well known [1] and reduces to a modulational instability analysis. The ansatz (3) is substituted into the NLS equation, the solution is linear-

ized around the reference solution E_{ref}, and terms of order 1 are collected:

$$i\frac{\partial q}{\partial z}+\frac{1}{2k_0}\Delta_\perp q+2\gamma I_0\mathrm{Re}(q)=0.$$

This linear equation can be solved in the Fourier domain. By separating the real and imaginary parts $q=q_r+iq_i$ we get in particular the expression of the real part q_r that characterizes the amplitude modulations in the linear regime, while q_i characterizes the phase modulations:

$$\hat{q}_r(z,\mathbf{k})=\cosh[g(\mathbf{k})z]\hat{q}_{0r}(\mathbf{k})+\frac{|\mathbf{k}|}{\sqrt{2k_c^2-|\mathbf{k}|^2}}\sinh[g(\mathbf{k})z]\hat{q}_{0i}(\mathbf{k}), \tag{4}$$

$$\hat{q}_i(z,\mathbf{k})=\frac{\sqrt{2k_c^2-|\mathbf{k}|^2}}{|\mathbf{k}|}\sinh[g(\mathbf{k})z]\hat{q}_{0r}(\mathbf{k})+\frac{|\mathbf{k}|}{\sqrt{2k_c^2-|\mathbf{k}|^2}}\cosh[g(\mathbf{k})z]\hat{q}_{0i}(\mathbf{k}), \tag{5}$$

where g is the linear growth rate,

$$g(\mathbf{k})=\frac{|\mathbf{k}|\sqrt{2k_c^2-|\mathbf{k}|^2}}{2k_0},$$

and $k_c=\sqrt{2\gamma k_0 I_0}$ corresponds to the maximum of the growth rate. As a result the real part of the modulation during the linear regime obeys Gaussian statistics with PSD

$$\Gamma_{q_r}(z,\mathbf{k})=\Gamma_{q_0}(\mathbf{k})h(\mathbf{k})\{\cosh[2g(\mathbf{k})z]+(1-|\mathbf{k}|^2/k_c^2)\}, \tag{6}$$

where $h(\mathbf{k})=k_c^2/(4k_c^2-2|\mathbf{k}|^2)$.

White noise. Let us address the case where the initial modulation is a white noise $\Gamma_{q_0}(\mathbf{k})\equiv\Gamma_0\ll 1$. The linear growth rate is maximal for wave vectors with modulus close to k_c. If $\gamma I_0 z>1$, then the PSD is maximal for wave numbers close to k_c and can be approximated by the Gaussian

$$\Gamma_{q_r}(z,\mathbf{k})\simeq\frac{1}{4}\Gamma_0\exp\left(\frac{k_c^2 z}{k_0}-\frac{(|\mathbf{k}|-k_c)^2 z}{k_0}\right).$$

Note that the width of the PSD is $\sqrt{k_0/z}$, which decays with increasing z. This spectral-gain-narrowing effect originates from the fact that wave numbers close to k_c grow much quicker than the other ones, so that the PSD after a transient period becomes independent of the initial PSD. Of course this holds true only if the initial perturbation contains modulations around k_c, as no new wavelength can be generated during the linear stage.

Exponentially decaying spectrum. Let us address the case where the initial modulation is a colored noise with PSD $\Gamma_{q_0}(\mathbf{k})\equiv\Gamma_0\exp(-|\mathbf{k}|/k_1)$ with $\Gamma_0\ll 1$. If $k_1\to\infty$, then we recover the white noise case. If k_1 is small, then the initial spectrum decays very fast so that low modes are initially dominant. High modes are progressively enhanced by the spectral gain. The dominant mode at some z results from the interplay of the exponential decay rate of the initial spectrum and the spectral gain selection. Indeed, the spectrum decays exponentially, while the gain factor is an exponential function of the wave number with entries that grow up with z. Explicit computations are possible. It is found that low modes are dominant until $z=z_1$, with $z_1=k_0/(\sqrt{2}k_c k_1)$. Then the wave number of the dominant mode of the modulation increases continuously in z from 0 to k_c:

$$k_p^2(z)=k_c^2\frac{4(z/z_1)^2-1-\sqrt{1+8(z/z_1)^2}}{4(z/z_1)^2}.$$

Discussion. It thus appears that two phenomena are in competition for the determination of the PSD. On the one hand, the initial modulation spectrum usually possesses a dominant spectral band. These dominant modes prevail during the early steps of the linear regime. On the other hand, the spectral gain curve tends to enhance the growth of the modes around k_c. If the linear stage is long enough, then this spectral selection eventually prevails and the dominant modes are those around k_c. This results in a loss of memory of initial conditions but the local rms of the initial modulation around k_c. The result of this competition turns out to involve dramatic effects to the WNL regime. Indeed this regime is characterized by mode coupling among the dominant modes. In this paper we mainly address initial modulations with low initial amplitudes, so that we focus our attention on the scenario with the strong spectral selection effect.

The modulation rms of q_r is

$$\sigma^2(z)=\frac{1}{(2\pi)^2}\int_{\mathbb{R}^2}\Gamma_{q_r}(z,\mathbf{k})d^2\mathbf{k}, \tag{7}$$

where Γ_{q_r} is given by Eq. (6). As shown in the subsequent sections this rms value turns out to be the key parameter. In case of strong spectral gain selection $\gamma I_0 z>1$, we can neglect transient terms of the form $\exp(-gz)$ in the conversion efficiency so that the expression of the modulation rms can be simplified into

$$\sigma^2(z)\simeq\frac{1}{4}\frac{1}{(2\pi)^2}\int_{\mathbb{R}^2}\Gamma_{q_0}(z,\mathbf{k})e^{2g(\mathbf{k})z}d^2\mathbf{k}. \tag{8}$$

In the case of a very strong spectral selection $\gamma I_0 z\gg 1$, the loss of memory of initial conditions becomes apparent as the expression of σ^2 can be further simplified into

$$\sigma^2(z)\simeq\sigma_0^2\left(\frac{k_c^2 z}{k_0}\right)^{-1/2}\exp\left(\frac{k_c^2 z}{k_0}\right), \tag{9}$$

where

$$\sigma_0^2=\frac{1}{8\pi^{3/2}}\int_C\Gamma_{q_0}(\mathbf{k})d^2\mathbf{k},$$

$$C=\{\mathbf{k}\in\mathbb{R}^2, 0.75k_c\leqslant|\mathbf{k}|\leqslant 1.25k_c\}. \tag{10}$$

The parameter σ_0^2 is proportional to the local rms of q_0 around the wave number k_c.

B. Third-order WNL analysis

A solution is sought in the form $E(z,\mathbf{r})=E_{ref}(z,\mathbf{r})[1+q(z,\mathbf{r})]$ where E_{ref} is the plane wave (2). Assuming that the

typical amplitude ε of the initial modulations is small, q can be expanded as

$$q(z,\mathbf{r}) = \varepsilon q_1(z,\mathbf{r}) + \varepsilon^2 q_2(z,\mathbf{r}) + \varepsilon^3 q_3(z,\mathbf{r}) + O(\varepsilon^4).$$

We then substitute this ansatz into the NLS equation, and we collect the terms with the same powers in ε. We obtain by collecting the terms of order ε the linear Bespalov-Talanov system starting from $q_1(z=0,\mathbf{r})=q_0(\mathbf{r})$. By collecting terms of order ε^{j+1}, $j\geqslant 1$, we obtain a series of linear systems for the jth-order perturbations. The second-order system reads as a linear system in q_2 with source terms quadratic in q_1:

$$i\frac{\partial q_2}{\partial z} + \frac{1}{2k_0}\Delta_\perp q_2 + 2\gamma I_0 \mathrm{Re}(q_2) = -\gamma I_0(q_1^2 + 2|q_1|^2),$$

$$q_2(z=0,\mathbf{r}) = 0. \tag{11}$$

The third-order system reads as a linear system in q_3 with source terms cubic in q_1:

$$i\frac{\partial q_3}{\partial z} + \frac{1}{2k_0}\Delta_\perp q_3 + 2\gamma I_0 \mathrm{Re}(q_3) = -\gamma I_0(2q_1 q_2 + |q_1|^2 q_1 + 2q_2^* q_1 + 2q_2 q_1^*),$$

$$q_3(z=0,\mathbf{r}) = 0. \tag{12}$$

A tractable approach is a weakly nonlinear analysis which consists in solving Eqs. (11) and (12) recursively. Qualitatively, terms of order ε^2 give the second-order nonlinear corrections. They involve sum-frequency and difference-frequency generations, but the fundamental modulations are not affected at this order. The nonlinear corrections to the fundamental modulations appear in the third-order perturbations in ε^3.

In the WNL framework the process q is not Gaussian anymore, but the calculations below show that we still have for $\mathbf{k},\mathbf{k}'\neq 0$:

$$\langle \hat{q}(z,\mathbf{k})\hat{q}(z,\mathbf{k}')\rangle = \Gamma(z,\mathbf{k})\delta_0(\mathbf{k}+\mathbf{k}').$$

The WNL analysis consists in expanding the modulation q with respect to its initial amplitude $\varepsilon \ll 1$, which reads in the Fourier domain as

$$\hat{q}(z,\mathbf{k}) = \varepsilon\hat{q}_1(z,\mathbf{k}) + \varepsilon^2\hat{q}_2(z,\mathbf{k}) + \varepsilon^3\hat{q}_3(z,\mathbf{k}) + O(\varepsilon^4),$$

where $\hat{q}_j(z,\mathbf{k})$ contains terms of the form $\hat{q}_0(\mathbf{k}_0)\cdots\hat{q}_0(\mathbf{k}_j)$, $\mathbf{k}_0+\cdots+\mathbf{k}_j=\mathbf{k}$. As a result moments of the form $\langle \hat{q}_j(z,\mathbf{k}')\hat{q}_{j'}(z,\mathbf{k})\rangle$ are zero if $j+j'$ is odd because they involve odd moments of the zero-mean Gaussian process $\hat{q}_0$. The physically relevant quantity is the PSD. The second moment of the Fourier modes can be expanded in powers of ε, and we get

$$\langle|\hat{q}(z,\mathbf{k})|^2\rangle = \underbrace{\varepsilon^2\langle|\hat{q}_1(z,\mathbf{k})|^2\rangle}_{\text{linear}} + \underbrace{\varepsilon^4[2\,\mathrm{Re}\langle\hat{q}_3(z,\mathbf{k})\hat{q}_1^*(z,\mathbf{k})\rangle + \langle|\hat{q}_2(z,\mathbf{k})|^2\rangle]}_{\text{WNL}} + O(\varepsilon^6). \tag{13}$$

This equation shows that the lowest-order WNL correction for the PSD is of order ε^4 and depends both on the second- and third-order terms of the WNL expansion. That is why it is necessary to develop a third-order WNL analysis to capture all effects of comparable magnitude in the multimode case.

The jth-order correction $q_j=q_{jr}+iq_{ji}$ is expanded in real and imaginary parts. A Fourier transform is applied with respect to the transverse spatial variables $\mathbf{r}$. In the strong-spectral-selection case, terms like $\cosh[g(\mathbf{k})z]$ and $\sinh[g(\mathbf{k})z]$ can be approximated by $(1/2)\exp[g(\mathbf{k})z]$ and we eventually get the following expression for the second-order correction:

$$\hat{q}_{2r}(z,\mathbf{k}) = \frac{1}{8\pi}\frac{4|\mathbf{k}|^2/k_c^2-4}{4-2|\mathbf{k}|^2/k_c^2+|\mathbf{k}|^4/k_c^4}\int d^2\mathbf{k}_1 e^{[g(\mathbf{k}_1)+g(\mathbf{k}-\mathbf{k}_1)]z}\check{q}_0(\mathbf{k}_1)\check{q}_0(\mathbf{k}-\mathbf{k}_1),$$

$$\hat{q}_{2i}(z,\mathbf{k}) = \frac{1}{8\pi}\frac{2|\mathbf{k}|^2/k_c^2+4}{4-2|\mathbf{k}|^2/k_c^2+|\mathbf{k}|^4/k_c^4}\int d^2\mathbf{k}_1 e^{[g(\mathbf{k}_1)+g(\mathbf{k}-\mathbf{k}_1)]z}\check{q}_0(\mathbf{k}_1)\check{q}_0(\mathbf{k}-\mathbf{k}_1),$$

where $\check{q}_0=\hat{q}_{0r}+\hat{q}_{0i}$. The expression of the third-order correction is quite complicated, so we only give a simplified expression valid when the modulus of $\mathbf{k}$ is close to k_c:

$$\hat{q}_{3r}(z,\mathbf{k}) = \frac{1}{64\pi^2}\int\int d^2\mathbf{k}_1 d^2\mathbf{k}_2 \frac{-8-(|\mathbf{k}_1+\mathbf{k}_2|^4)/k_c^4}{4-2(|\mathbf{k}_1+\mathbf{k}_2|^2)/k_c^2} + (|\mathbf{k}_1+\mathbf{k}_2|^4)/k_c^4 \times e^{[g(\mathbf{k}_1)+g(\mathbf{k}_2)+g(\mathbf{k}-\mathbf{k}_1-\mathbf{k}_2)]z}\check{q}_0(\mathbf{k}_1)\check{q}_0(\mathbf{k}_2)\check{q}_0(\mathbf{k}-\mathbf{k}_1-\mathbf{k}_2),$$

$$\hat{q}_{3i}(z,\mathbf{k}) = \frac{1}{64\pi^2}\int\int d^2\mathbf{k}_1 d^2\mathbf{k}_2 \frac{-8+16(|\mathbf{k}_1+\mathbf{k}_2|^2)/k_c^2+(|\mathbf{k}_1+\mathbf{k}_2|^4)/k_c^4}{4-2(|\mathbf{k}_1+\mathbf{k}_2|^2)/k_c^2+(|\mathbf{k}_1+\mathbf{k}_2|^4)/k_c^4} \times e^{[g(\mathbf{k}_1)+g(\mathbf{k}_2)+g(\mathbf{k}-\mathbf{k}_1-\mathbf{k}_2)]z}\check{q}_0(\mathbf{k}_1)\check{q}_0(\mathbf{k}_2)\check{q}_0(\mathbf{k}-\mathbf{k}_1-\mathbf{k}_2).$$

Substituting into Eq. (13) we obtain that the PSD has the following form for $\mathbf{k}\neq 0$ in the WNL regime:

$$\Gamma(z,\mathbf{k}) = \varepsilon^2 W_1(z,\mathbf{k})\Gamma_{q_0}(\mathbf{k}) + \frac{\varepsilon^4}{(2\pi)^2}\int d^2\mathbf{k}_1 W_2(z,\mathbf{k},\mathbf{k}_1)\Gamma_{q_0}(\mathbf{k}_1)\Gamma_{q_0}(\mathbf{k}-\mathbf{k}_1) + \frac{\varepsilon^4}{(2\pi)^2}\int d^2\mathbf{k}_1 W_3(z,\mathbf{k},\mathbf{k}_1)\Gamma_{q_0}(\mathbf{k}_1)\Gamma_{q_0}(\mathbf{k}), \quad (14)$$

where W_1 is the growth rate of the mode with wave number $\mathbf{k}$. W_2 [W_3] depends on the conversion efficiency of the sum frequency generation $\mathbf{k}_1+(\mathbf{k}-\mathbf{k}_1)\rightarrow[\mathbf{k}_1+(-\mathbf{k}_1)+\mathbf{k}\rightarrow\mathbf{k}]$. They have complicated expressions but they can be simplified if $k_c^2 z/k_0 \gg 1$ because transient components can be neglected:

$$W_1(z,\mathbf{k}) = \frac{1}{2}\exp[2g(\mathbf{k})z],$$

$$W_2(z,\mathbf{k},\mathbf{k}_1) = \frac{8-4|\mathbf{k}|^2/k_c^2+5|\mathbf{k}|^4/k_c^4}{2(4-2|\mathbf{k}|^2/k_c^2+|\mathbf{k}|^4/k_c^4)^2} \times\exp\{2[g(\mathbf{k}_1)+g(\mathbf{k}-\mathbf{k}_1)]z\},$$

$$W_3(z,\mathbf{k},\mathbf{k}_1) = \frac{-12+10(|\mathbf{k}+\mathbf{k}_1|^2)/k_c^2-(|\mathbf{k}+\mathbf{k}_1|^4)/k_c^4}{4[4-2(|\mathbf{k}+\mathbf{k}_1|^2)/k_c^2+(|\mathbf{k}+\mathbf{k}_1|^4)/k_c^4]} \times\exp\{2[g(\mathbf{k}_1)+g(\mathbf{k})]z\}.$$

The WNL analysis carried out in this section is somewhat similar to the weak turbulence (WT) description of the NLS equation [18]. The purpose of the WT theory is to write a closed-form equation for the second moment Γ, which requires one to estimate the fourth-order moment through the second moment. This key estimate is the building block of the WT theory [22]. Usually the WT theory for the NLS equation has the form of a kinetic equation with cubic nonlinearity ([18], Sec. II). However, the kinetic theory applied to the background of the plane-wave solution also exhibits quadratic terms similar to Eq. (14), as explained in [18] (Sec. IV).

IV. INTENSITY DISTRIBUTION

The powers of the intensity $I(z,\mathbf{r})^n$, with $n\in\mathbb{R}^+$, can be expanded as powers of ε:

$$I^n = I_0^n\{1+\varepsilon 2n\,\mathrm{Re}(q_1)+\varepsilon^2[2n\,\mathrm{Re}(q_2)+n(n-1)\mathrm{Re}(q_1^2)+n^2|q_1|^2]+O(\varepsilon^3)\}.$$

The first moment ($n=1$) can be computed directly from the energy conservation $\langle I\rangle = I_0$, which implies $\langle q_{1r}\rangle = 0$, $2\langle q_{2r}\rangle + \langle|q_1|^2\rangle = 0$. These identities can also be obtained from the complete expressions of q_1 and q_2. The nth-order moment is

$$\langle I^n\rangle = I_0^n[1+\varepsilon^2 n(n-1)\langle|q_1|^2\rangle + O(n^4\varepsilon^4)].$$

We shall compute the term of order $n^4\varepsilon^4$ in the next paragraph. From this collection of expansions we can propose a consistent representation of the nth moment which reads as

$$\langle I^n\rangle = I_0^n\exp[2n(n-1)\sigma^2(z)],$$

where σ is the modulation rms computed in the linear regime and given by Eq. (7). The application of an inverse Laplace transform then yields the expression of the probability density function (PDF) of the intensity:

$$p_z(I) = \frac{\sqrt{I_0}}{2^{3/2}\pi^{1/2}I^{3/2}\sigma(z)}\exp\left(-\frac{\sigma^2(z)}{2}-\frac{\ln(I/I_0)^2}{8\sigma^2(z)}\right). \quad (15)$$

If the modulation rms is very small, $\sigma(z)\ll 1$, the PDF is approximately Gaussian with mean I_0 and variance $(2\sigma I_0)^2$. When σ becomes larger than 0.1, formula (15) shows that the departure from the Gaussian fit becomes significant, the PDF becomes asymmetric, and in particular the PDF tail corresponding to large values is much heavier than a Gaussian (see Fig. 1). This decay rate is still larger than any power, but it is slower than any exponential. This demonstrates a departure from the Gaussian fit. Furthermore, the mean intensity is still I_0, so that the PDF peak is shifted to a value lower than I_0.

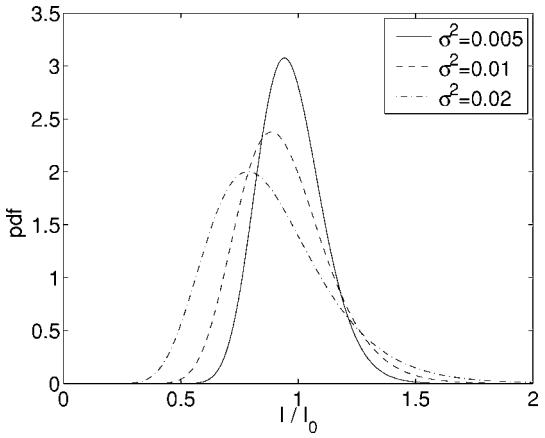

FIG. 1. Intensity distribution for different values of $\sigma^2(z)$.

The contrast is a dimensionless parameter that characterizes the relative fluctuations of the intensity. It is defined by

$$c^2 = \frac{\langle I^2\rangle - \langle I\rangle^2}{\langle I\rangle^2}.$$

Using the expansions derived in the previous sections, we get that the first moments of the intensity are $\langle I\rangle = I_0$, $\langle I^2\rangle = I_0^2[1+2\varepsilon^2\langle|q_1|^2\rangle + O(\varepsilon^4)]$, which shows that the expansion of the contrast at second order is

$$c^2 = 4\sigma(z)^2 + O(\sigma^4(z)). \quad (16)$$

The expansion can be extended to higher orders. The intensity reads

$$I = I_0\{1+2\varepsilon q_{1r}+\varepsilon^2(2q_{2r}+|q_1|^2)+\varepsilon^3[2q_{3r}+2\,\mathrm{Re}(q_1 q_2^*)] + \varepsilon^4[2q_{4r}+2\,\mathrm{Re}(q_1 q_3^*)+|q_2|^2]+O(\varepsilon^5)\},$$

where q_{jr} (q_{ji}) stands for the real (imaginary) part of the jth term q_j. It seems that we should know the fourth-order correction q_{4r}, but we can compute the fourth-order correction

to the moments of I without it. Indeed, energy conservation imposes $\langle I\rangle = I_0$, so that $2\langle q_{4r}\rangle + 2\langle \mathrm{Re}(q_1 q_3^*)\rangle + \langle |q_2|^2\rangle = 0$, and thus we can write

$$\langle I^2\rangle = I_0^2\{1 + 4\varepsilon^2\langle |q_1|^2\rangle + \varepsilon^4[8\langle q_{1r}q_{3r}\rangle + 4\langle q_{2r}^2\rangle + 4\langle q_{2r}|q_1|^2\rangle + 8\langle \mathrm{Re}(q_2 q_1^*)q_{1r}\rangle + \langle |q_1|^4\rangle] + O(\varepsilon^6)\}. \quad (17)$$

The fourth-order moments of Gaussian processes can be expressed as products of second-order moments, so that long but straightforward algebra yields

$$c^2 = 4\sigma^2(z) + K_4\sigma^4(z) + O(\sigma^6(z)),$$

with $K_4 = 8[-1 + \sqrt{2}(8\times 3^{-3/4} - 3^{-1/4})] \simeq 24$. We can identify this expansion as the Taylor expansion of

$$c^2 = \frac{1}{\sqrt{1 - 8\sigma^2(z)}} - 1, \quad (18)$$

and we shall use from now on this expression.

V. GROWTH OF THE LOCAL MAXIMA

A. Joint distribution of the local maxima in the linear regime

We first address the linear regime of exponential growth of the modes. We consider a transverse beam section with surface S located at a propagation distance z from the initial plane. The process $(q_r(\mathbf{r}))_{\mathbf{r}\in S}$ has Gaussian statistics; its power spectral density is known and presents a maximum around the optimal wave number k_c. We aim at studying the values of the local maxima of this process, which impose the local peak intensities of the hot spots of the transverse beam profile. Note that this problem was addressed in Ref. [23] in the case of a speckle pattern modeled by a complex Gaussian process. Here the process q_r is real valued and its PSD has a very particular structure that allows us to push forward the analysis.

We denote by $(q_1, q_2, \ldots, q_n)$ the values of the n largest local maxima of q_r. The strategy follows the same line as the one used in Ref. [23]; it is based on mathematical results about extrema of Gaussian processes [20]. We get that the statistical distribution of this vector can be described as

$$q_j = \sqrt{2}\sigma(z)[M_D - \ln(X_1 + \cdots + X_j)]^{1/2}, \quad j = 1, \ldots, n, \quad (19)$$

where

$$M_D = \ln(D) + \frac{1}{2}\ln[\ln(D)], \quad D = \frac{k_p^2(z)S}{4\pi^{3/2}}, \quad (20)$$

where $\sigma(z)$ is given by Eq. (7), $k_p(z)$ is the carrier wave number of the PSD of q_r,

$$k_p^2(z) = \frac{\int |\mathbf{k}|^2 \Gamma_{q_r}(z,\mathbf{k}) d^2\mathbf{k}}{\int \Gamma_{q_r}(z,\mathbf{k}) d^2\mathbf{k}},$$

and $(X_j)_{1\leqslant j\leqslant n}$ is a collection of independent and identically distributed random variables with an exponential probability density function with mean 1. In terms of the beam intensity, these local maxima correspond to hot spots with peak intensities

$$I_j = I_0 \exp(2q_j), \quad (21)$$

where the exponential has been chosen consistently with the predictions of the WNL approach. In the case of a strong spectral selection, $\sigma(z)$ is given by Eq. (8) and $k_p(z) = k_c = \sqrt{2\gamma k_0 I_0}$.

We have just determined the values of the peak intensities of the hot spot. The evolution of a hot spot also depends on the local intensity profile and, in particular, the power carried by the hot spot. This power can be estimated from the effective area S_e of the hot spot, so that the hot spot power is $I_0 S_e$. From the expression of the PSD, the field modulation is dominated by the wave number $k_c = \sqrt{2\gamma I_0 k_0}$. More exactly, the autocorrelation function of the field q_r is the Fourier transform of the PSD so that it has the form $C(x) \simeq J_0(k_c|x|)C(0)$. A theorem that can be found in the monography by Adler [20] then states that the typical local profile of the Gaussian field close to a local maximum located in $\mathbf{r}_0$ is imposed by the autocorrelation function and has the form $q_r(\mathbf{r}) = q_r(\mathbf{r}_0)J_0(k_c|\mathbf{r}-\mathbf{r}_0|)$. Accordingly the effective area of the hot spot is the surface of a disk with radius $r_0 = \alpha_0/k_c$ where α_0 is the first zero of the Bessel function J_0: $\alpha_0 \simeq 2.405$. This result is in qualitative agreement with previous estimates[19,24] which did not use the form of the autocorrelation function and Adler's theorem. The hot spot power can thus be estimated by $P_0 = I_0\pi\alpha_0^2/k_c^2$, or else $P_0 = (\alpha_0^2\pi)/(2\gamma k_0)$. As a result, the intensity of a hot spot increases with z and eventually reaches the value $2I_0$ where the hot spot can be described as a Gaussian beam with radius r_0, whose power is P_0.

B. Independent hot spot approach in the fully nonlinear regime

The WNL analysis is not valid anymore when the maximal intensity I_{max} becomes too large (i.e., when $I_{max} - I_0 \sim I_0$). Note that most of the beam is still in the WNL regime when the maximal intensity reaches the level $2I_0$. This means that the formulas for the contrast and energy distribution still hold true, but a fully nonlinear approach is required for a description of the most intense hot spots. The idea is then to switch from the WNL result (19)–(21) to formulas describing the self-focusing of isolated hot spots. This analysis will be called in the following the "independent hot spot" approach. It is crucial to determine the transition from the WNL regime to the FNL regime to capture the effective dynamics of hot spots.

Let us first consider the hottest spot. Its peak intensity reaches the value $2I_0$ after a propagation distance z_0 such that $\sqrt{2}\sigma(z_0)[M_D - \ln(X_1)]^{1/2} = \sigma_1$ with $\sigma_1 = \ln(2)/2 \simeq 0.35$. This characteristic distance can be studied more precisely in case of a strong spectral selection, when $\sigma^2(z)$ has the form (9). As a result z_0 can be written as

$$z_0 = \bar{z}_0 + \frac{k_0}{k_c^2 M_D} Z,$$

where

$$\bar{z}_0 = \frac{k_0}{k_c^2}\left[\ln\left(\frac{\ln(2)^2}{8M_D\sigma_0^2}\right) + \frac{1}{2}\ln\ln\left(\frac{\ln(2)^2}{8M_D\sigma_0^2}\right)\right] \quad (22)$$

and Z is a random variable with probability density function $p(z)=\exp[z-\exp(z)]$. Note that the left PDF tail corresponding to the occurrence of small values of z_0 decays as an exponential. This tail is important because it is responsible for unexpected filamentation events at small propagation distances. However, the deterministic component $\bar{z}_0$ is usually much larger than the random component (in the asymptotic $M_D \gg 1$). In a first crude approximation we may thus assume that $z_0 \simeq \bar{z}_0$.

Once the peak intensity has reached the value $2I_0$, we consider that the hot spot behaves like a Gaussian pulse with initial intensity $2I_0$ and radius r_0. The following dynamics is then fully deterministic. Standard results of the self-focusing of Gaussian beams are available [19,25]. Note that the power of the hot spot is above the critical power for self-focusing, $\mathcal{P}_0 \simeq 1.55\mathcal{P}_c$. Here the critical power is the power of the so-called Townes soliton, $\mathcal{P}_c = \pi N_c/(\gamma k_0)$, $N_c \simeq 1.862$ [26]. Numerical studies confirm that we can adopt the following ansatz for the growth of the peak intensity of the hot spot (for $z > z_0$):

$$I(z) = \frac{I_0}{0.5 - 0.347\gamma I_0 (z - z_0) - 0.05\gamma^2 I_0^2 (z - z_0)^2}. \quad (23)$$

Note that the transition from the WNL regime to the FNL regime for the hot spot is smooth in the sense that the function $z \mapsto I(z)$ is continuous and continuously differentiable in z_0. This was actually one of the requirements for the choice of the ansatz (23). There exists a random component in $I(z)$, which originates from the fact that z_0 is random. In a first approximation we can take $z_0 = \bar{z}_0$. This expression is in agreement with well-known empirical expressions for a blowup of Gaussian initial conditions (see, for instance, [25], Sec. 7.3.1 and references therein).

As a summary, if $z \leqslant \bar{z}_0$, the maximal intensity is approximately

$$I_{max}(z) = I_0 \exp[2\sqrt{2}\sigma(z)\sqrt{M_D}], \quad (24)$$

with $\sigma(z)$ given by Eq. (7), M_D defined by Eq. (20), and $\bar{z}_0$ by Eq. (22).

If $\bar{z}_0 \leqslant z \leqslant \bar{z}_0 + z_f$, $z_f = 1.1/(\gamma I_0)$, then the maximal intensity is

$$I_{max}(z) = \frac{I_0}{0.5 - 0.347\gamma I_0 (z - \bar{z}_0) - 0.05\gamma^2 I_0^2 (z - \bar{z}_0)^2}. \quad (25)$$

Finally, if $z > z_f + \bar{z}_0$, then $\bar{I}(z) \geqslant 15 I_0$ which means that the hottest spot has just blown up or is about to blow up. We know that in such a case the NLS equation is not valid anymore, and this means for us that optical damage will occur.

C. Number of filaments

In this subsection we give the statistical distribution of the number of filaments whose peak intensities are larger than some value of the form αI_0, $\alpha > 1$. This number is denoted by N_α, and it can be described in terms of a Poisson distribution. Let us first give some well-known features about the Poisson distribution. A random variable N obeys a Poisson distribution with parameter $\lambda > 0$ if its state space is the set of non-negative integers and $\mathbb{P}(N=k) = \exp(-\lambda)\lambda^k/k!$, $k \in \mathbb{N}$. Its expectation is λ, and its variance is also λ. If $\lambda \ll 1$, then $\mathbb{P}(N=0) \simeq 1 - \lambda + O(\lambda^2)$, $\mathbb{P}(N=1) = \lambda + O(\lambda^2)$, and $\mathbb{P}(N \geqslant 2) = O(\lambda^2)$. If $\lambda \gg 1$, then the Poisson distribution can be fitted by a Gaussian distribution with mean λ and variance λ.

Let us first address the statistical distribution of N_α for $\alpha \in (1,2]$. This distribution is imposed by the results obtained in the WNL regime, when we know that the first n local maxima have peak intensities described by the formula (21). It is then straightforward to establish that N_α obeys a Poisson distribution with parameter

$$\lambda_\alpha = \exp\left(M_D - \frac{\ln^2(\alpha)}{8\sigma^2(z)}\right).$$

Let us now address the statistical distribution of N_α for $\alpha \in [2,16]$. The results obtained in the FNL regime are then useful. We find that N_α obeys a Poisson distribution with parameter

$$\lambda_\alpha = \exp\left[M_D - \frac{\ln(2)^2}{8\sigma^2(z)}\exp[2f(\alpha)]\right],$$

where $f(\alpha) = -3.47 + \sqrt{3.47^2 + 10(1 - 2/\alpha)} \simeq (0.5 - 1/\alpha)/0.347$.

VI. DISCUSSION

A. Role of the initial spectrum

If the input noise has a small variance, then the linear regime is long enough so that the spectral gain selection eventually prevails. This results in a loss of memory of initial conditions, and the dominant modes are those with wave numbers around k_c. The WNL regime then depends only on the effective parameter σ_0^2 defined by Eq. (10) as the local rms of the initial modulation around wave number k_c.

If the input noise has a strong enough variance, then the picture is very different. The linear regime is short or even absent, and some modes reach amplitudes that excite WNL effects before the modes around k_c. The formulas for the contrast and intensity distributions still hold true if we take care to compute the parameter σ with the complete formula (7) that depends on the complete PSD of the input noise. The integral (7) is usually easy to compute especially in the usual case where noise is isotropic so that the PSD depends only on the wave number and not the wave vector. However, the formula for the maximal intensity in the FNL regime is not likely to hold true because the dominant modes are not those around k_c, so that the ansatz for the intensity growth of the hottest spot could be wrong.

B. Extension beyond the plane-wave approximation

We have considered so far that the electric field is a plane wave to leading order. In this subsection we extend the results to the case where the input beam possesses (1) a well-defined slowly varying envelope with spatial radius R_0 (the so-called beam radius) and (2) small-scale small-amplitude random modulations with characteristic scale ρ_0 (the so-called correlation radius). By introducing the typical nonlinear length scale $r_c=(2\gamma k_0 I_0)^{-1/2}$, where I_0 is the typical beam intensity, the forthcoming analysis is based on a separation-of-scales technique $\rho_0 \leqslant r_c \ll R_0$. We also assume that the propagation distance Z is of the order of a few nonlinear distances $(\gamma I_0)^{-1}$. As a result, in the absence of small modulations, the beam propagates without deformation and only experiences self-phase modulation. In the presence of small modulations, small-scale structures emerge. The analysis follows the same line as in the plane-wave configuration, at the expense of splitting the beam into macrocells where the local plane-wave approximation can be done. We focus our attention on the intensity distribution. The intensity distribution of the transverse profile of the beam over a section S is defined as

$$\frac{1}{S}\text{area}(\mathbf{r} \in S, |E|^2(z,\mathbf{r}) \in [I_a, I_b]) = \int_{I_a}^{I_b} p_z(I)dI,$$

where p_z is the probability density function:

$$p_z(I) = \frac{1}{S}\int_S p_{z,I_0(\mathbf{r})}(I)d^2\mathbf{r}, \tag{26}$$

$$p_{z,I_0}(I) = \frac{\sqrt{I_0}}{2^{3/2}\pi^{1/2}I^{3/2}\sigma(z,I_0)}\exp\left(-\frac{\sigma^2(z,I_0)}{2} - \frac{\ln(I/I_0)^2}{8\sigma^2(z,I_0)}\right), \tag{27}$$

$$\sigma^2(z,I_0) = \frac{1}{(2\pi)^2}\int \Gamma(z,I_0,\mathbf{k})d^2\mathbf{k}. \tag{28}$$

The computation of the PSD Γ is straightforward. Here we assume that the initial phase and amplitude modulations may have different PSD that we denote by Γ_p and Γ_a, respectively. Indeed the input modulations are often dominated by phase modulations in practical configurations. We then have

$$\Gamma(\mathbf{k},I_0,z) = \Gamma_p(\mathbf{k})\frac{|\mathbf{k}|^2}{4\gamma k_0 I_0 - |\mathbf{k}|^2}\sinh^2[g_{I_0}(\mathbf{k})z] + \Gamma_a(\mathbf{k})\cosh^2[g_{I_0}(\mathbf{k})z],$$

where $g_{I_0}(\mathbf{k}) = |\mathbf{k}|\sqrt{4\gamma k_0 I_0 - |\mathbf{k}|^2}/(2k_0)$ and the substitution of this function into Eqs. (26) and (27) gives the intensity PDF.

VII. NUMERICAL SIMULATIONS

We carry out full numerical simulations of the NLS equation by a split-step Fourier method. We address the dimensionless version $k_0=1$, and $\gamma=1$, $I_0=1$, and we consider an initial noise with Gaussian autocorrelation function and PSD

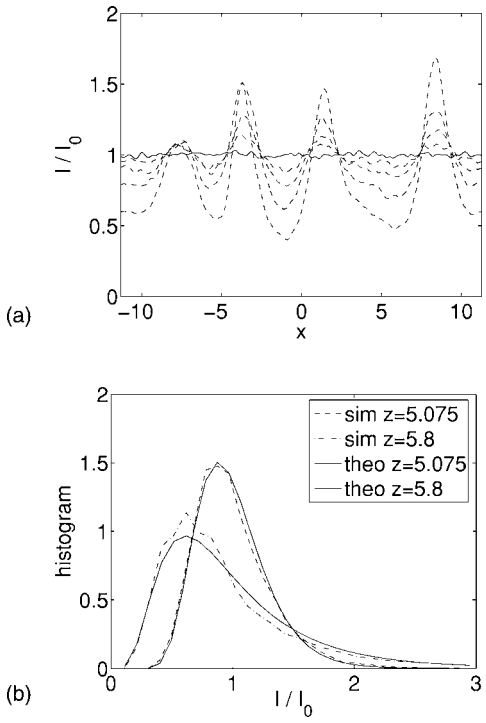

FIG. 2. (a) Intensity profile along an arbitrary line for the initial beam profile $z=0$ (solid line) and the beam profiles for $z=3.25$, $z=3.9$, $z=4.55$, and $z=5.2$ (dashed lines). (b) Intensity histograms (dashed and dot-dashed lines) and theoretical distributions (solid lines). Here $\sigma_0=10^{-2}$ and $r_c=0.2$.

$$\langle q_0(\mathbf{r}'+\mathbf{r})q_0(\mathbf{r}')\rangle = \sigma_0^2\exp\left(-\frac{|\mathbf{r}|^2}{2r_c^2}\right),$$

$$\Gamma_{q_0}(\mathbf{k}) = 2\pi\sigma_0^2 r_c^2\exp\left(-\frac{|\mathbf{k}|^2 r_c^2}{2}\right),$$

respectively. We take $r_c=0.2$ and different values for σ_0. This input noise is broadband in the sense that the initial PSD is much broader than the optimal wave number of the gain curve $k_c=\sqrt{2}$. In the numerical simulations the section of the beam profile has area 512. The total beam power is accordingly 90 times the critical power $\mathcal{P}_c$, and a propagation distance of 1 corresponds to a breakup integral (i.e., an accumulated nonlinear phase) of 1. The theoretical values are given by Eq. (18) for the contrast, Eq. (15) for the intensity distribution, and Eqs. (24) and (25) for the maximal intensity. All these values depend only on the parameter σ^2 given by Eq. (7).

In Figs. 2–4 the theoretical and numerical intensity histograms, contrasts, and maximal intensities are compared for $\sigma_0=10^{-2}$ and $\sigma_0=10^{-3}$, which shows very good agreement. In particular we can check that the formula (18) for the contrast accurately predicts the numerical contrast up to $c\simeq 1$. The WNL analysis thus allows us to go far beyond the linear regime where the modulation instability theory is valid. Practically, these figures show that, for the broadband modulation spectrum considered in this section, the beam can propagate

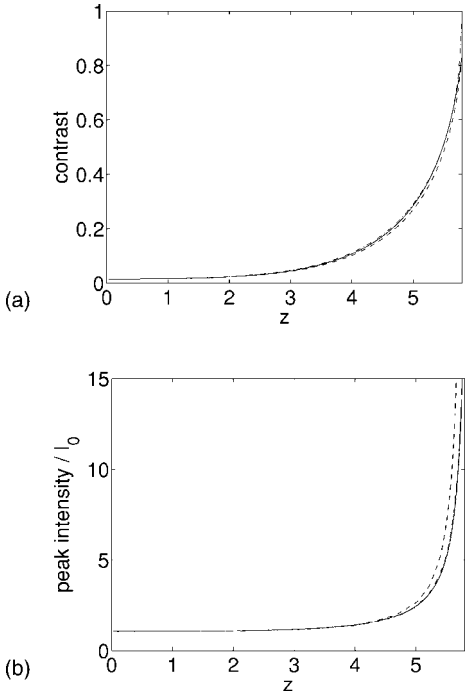

FIG. 3. (a) Contrast of the intensity distribution. Comparison between two numerical simulations (dashed and dot-dashed lines) and theory (solid line). (b) Maximal value of the intensity profile. Here $\sigma_0=10^{-2}$ and $r_c=0.2$.

without self-focusing over a propagation distance which corresponds to a breakup integral of 5 if the initial standard deviation is less than 1%.

Let us now consider two cases where the theoretical predictions are not very good. According to the above discussion this occurs when the input noise has a large variance so that the linear regime is very short or even absent; as a result, the beam modulations enter the FNL regime before spectral gain selection is able to enhance the modes around k_c. Practically, this means that the initial modulations present local maxima that are initially of order 1. The formulas for the contrast and intensity distribution can still be applied because the most important part of the beam follows the dynamics described in this paper consisting of a linear regime followed by a WNL regime. However, the theoretical formula for the maximal intensity is likely to be wrong because the initial global maximum immediately enters the FNL regime, so the result depends on the exact realization of the input noise, and not only its statistical distribution. In Fig. 5, $\sigma_0=0.05$, we can check that this configuration is at the border of the domain of validity of our theory. The theoretical predictions for the contrast and intensity distribution are still in agreement with the results of the simulations, but we can observe a non-negligible numerical volatility for the maximal intensity in the sense that the numerical results vary from one simulation to another one, meaning that the result depends on the particular realization of the input noise and not only its statistics. This volatility (or unpredictability) becomes all the more important as the initial noise variance is larger. In Figs. 6 and 7, $\sigma_0=0.1$ and the maximal intensity is initially around $2I_0$. We can then check that the theoretical predictions for the contrast and intensity distributions are correct, but the prediction for the maximal intensity is wrong. Practically, Figs. 5 and 6 show that the beam undergoes self-focusing if the breakup integral is larger than 3 and if the initial standard deviation is larger than a few percent.

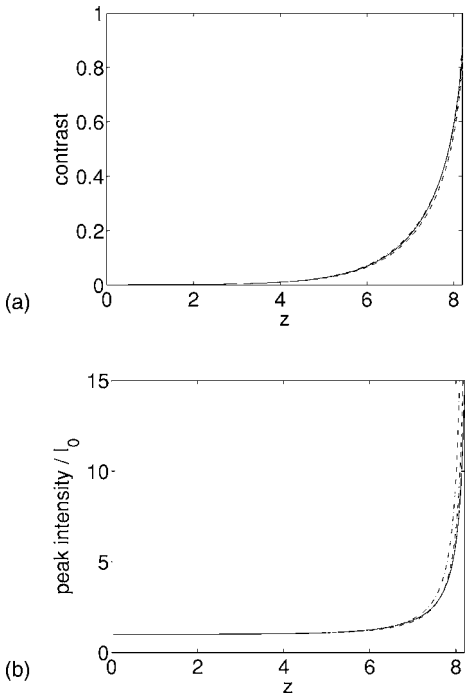

FIG. 4. Contrast (a) and maximal value (b) of the intensity profile. Here $\sigma_0=10^{-3}$ and $r_c=0.2$.

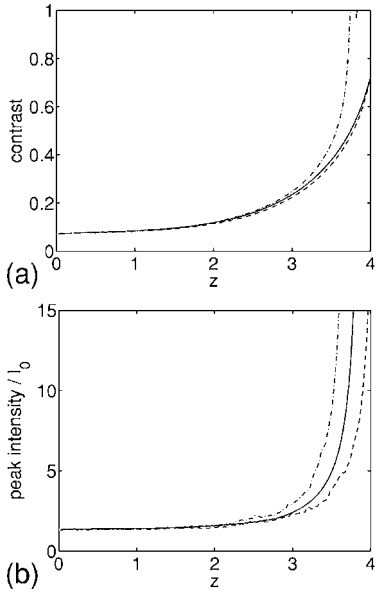

FIG. 5. Contrast (a) and maximal value (b) of the intensity profile. Here $\sigma_0=5\times10^{-2}$ and $r_c=0.2$.

VIII. CONCLUSION

In this paper we have studied the growth of intensity modulations for a large-aperture high-power laser beam in a

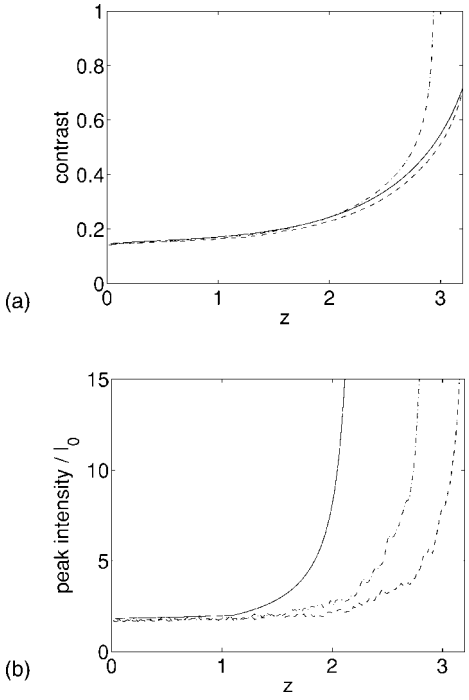

FIG. 6. Contrast (a) and maximal value (b) of the intensity profile. Here $\sigma_0=10^{-1}$ and $r_c=0.2$.

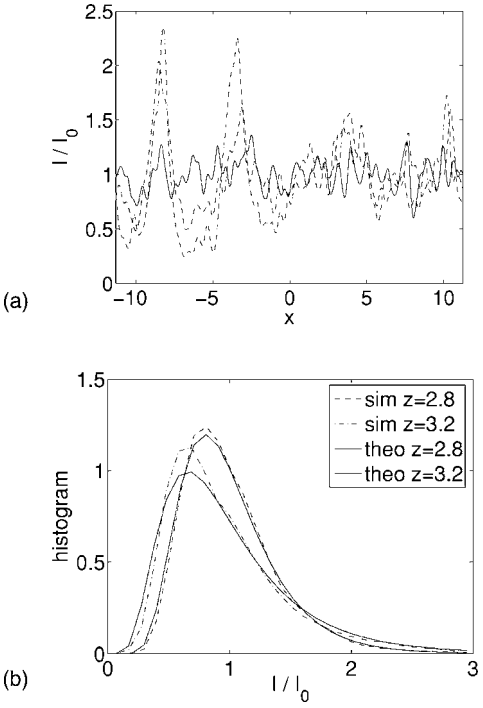

FIG. 7. (a) Intensity profile along an arbitrary line for the initial beam profile $z=0$ (solid line) and the beam profiles for $z=2.4$ and $z=3.2$ (dashed lines). (b) Intensity histograms (dashed and dot-dashed lines) and theoretical distributions (solid lines). Here $\sigma_0=10^{-1}$ and $r_c=0.2$.

Kerr medium. The multiple filamentation of the beam is triggered by noise in the input transverse profile, in both phase and amplitude. We use a description of the noise in terms of a Gaussian random process, and we characterize the filamentation process in terms of the initial power spectral density of the field modulations. The dynamics can be decomposed into three stages. First a linear stage involves the exponential growth of transverse modes. This stage enhances the modes around a particular wave number imposed by the input power. When the local modulation rms around the dominant modes reaches a critical value, coupling effects between modes speed up the modulation growths. This weakly nonlinear regime is transient and imposes initial conditions for the fully nonlinear regime. This final regime is characterized by the growth of quasi-isolated hot spots, and it can be described by an independent hot spot model.

This paper is devoted to one of the possible causes of filamentation. Recent studies have addressed other causes, such as vectorial effects [27]. These effects can be responsible for filamentation in the case where the beam power is larger than the critical power by a factor of the order of 10. For very high power noise-induced filamentation is the dominant phenomenon [14,15]. This paper gives a statistical quantitative analysis and allows us to predict the filamentation of laser beams in very-high-power laser chains.

[1] V. I. Bespalov and V. I. Talanov, JETP Lett. **3**, 471 (1966); [JETP Lett. **3**, 307 (1966)].
[2] R. G. Brewer and J. R. Lifsitz, Phys. Lett. **23**, 79 (1966).
[3] A. Brodeur, F. A. Ilkov, S. L. Chin, O. G. Kosareva, and V. P. Kandidov, Opt. Lett. **22**, 304 (1997).
[4] V. V. Korobkin and R. V. Serov, JETP Lett. **6**, 642 (1967); [JETP Lett. **6**, 135 (1967)].
[5] G. J. Lord, Phys. Rev. Lett. **22**, 994 (1969).
[6] V. Nowak and D. O. Ham, Opt. Lett. **6**, 185 (1981).
[7] A. V. Mamaev, M. Saffman, D. Z. Anderson, and A. A. Zozulya, Phys. Rev. A **54**, 870 (1996).
[8] J. Schwartz, P. Rambo, J. C. Diels, M. Kolesik, E. M. Wright, and J. V. Moloney, Opt. Commun. **180**, 383 (2000).
[9] M. Mlejnek, M. Kolesik, J. V. Moloney, and E. M. Wright, Phys. Rev. Lett. **83**, 2938 (1999).
[10] K. Konno and H. Suzuki, Phys. Scr. **20**, 382 (1979).
[11] H. Bercegol, P. R. Bouchut, L. Lamaignère, B. Le Garrec, and G. Razé, Proc. SPIE **5273**, 111 (2002).
[12] H. Bercegol, T. Donval, B. Forestier, L. Lamaignere, M. Loiseau, and G. Razé, Proc. SPIE **5647**, 355 (2005).
[13] P. M. Lushnikov and H. A. Rose, e-print physics/0512271.
[14] D. Milam, J. T. Hunt, K. R. Manes, and W. H. Williams, Proc. SPIE **2966**, 425 (1997).
[15] W. H. Williams, K. R. Manes, J. T. Hunt, P. A. Reynard, D. Milam, and D. Eimerl, UCRL-LR-105821–96–1, ICF Quart. Rep. **6**(1), 7–14 (Lawrence Livermore National Laboratory, Livermore, CA, 1995).
[16] J. H. Marburger and E. Dawes, Phys. Rev. Lett. **21**, 556

(1968).
[17] A. J. Campillo, S. L. Shapiro, and B. R. Suydam, Appl. Phys. Lett. **23**, 628 (1973).
[18] S. Dyachenko, A. C. Newell, A. Pushkarev, and V. E. Zakharov, Physica D **57**, 96 (1992).
[19] J. H. Marburger, Prog. Quantum Electron. **4**, 35 (1975).
[20] R. Adler, *The Geometry of Random Fields* (Wiley, New York, 1981).
[21] M. D. Feit and J. A. Fleck, J. Opt. Soc. Am. B **5**, 633 (1998).
[22] V. E. Zakharov, S. L. Musher, and A. M. Rubenchik, Phys. Rep. **129**, 285 (1985).
[23] J. Garnier, C. Gouédard, and A. Migus, J. Mod. Opt. **46**, 1213 (1999).
[24] L. Bergé, M. R. Schmidt, J. J. Rasmussen, P. L. Christiansen, and K. O. Rasmussen, J. Opt. Soc. Am. B **14**, 2550 (1997).
[25] G. Fibich and G. Papanicolaou, SIAM J. Appl. Math. **60**, 183 (1999).
[26] M. Weinstein, Commun. Math. Phys. **87**, 567 (1983).
[27] G. Fibich and B. Ilan, Physica D **157**, 112 (2001).